

## ***Velvet*, a Dominant *Egfr* Mutation That Causes Wavy Hair and Defective Eyelid Development in Mice**

**Xin Du,\* Koichi Tabeta,\* Kasper Hoebe,\* Haiquan Liu,<sup>†</sup> Navjiwan Mann,\* Suzanne Mudd,\*  
Karine Crozat,\* Sosathya Sovath,\* Xiaohua Gong<sup>†</sup> and Bruce Beutler\*<sup>1</sup>**

\*Department of Immunology, Scripps Research Institute, La Jolla, California 92037 and <sup>†</sup>School of Optometry and Vision Science Program, University of California, Berkeley, California 94720

Manuscript received July 9, 2003

Accepted for publication September 24, 2003

### ABSTRACT

In the course of a large-scale program of ENU mutagenesis, we isolated a dominant mutation, called *Velvet*. The mutation was found to be uniformly lethal to homozygotes, which do not survive E13.5. Mice heterozygous for the *Velvet* mutation are born with eyelids open and demonstrate a wavy coat and curly vibrissae. The mutation was mapped to the proximal end of chromosome 11 by genome-wide linkage analysis. On 249 meioses, the locus was confined to a 2.7-Mb region, which included the epidermal growth factor receptor gene (*Egfr*). An A → G transition in the *Egfr* coding region of *Velvet* mice was identified, causing the amino acid substitution D833G. This substitution alters an essential triad of amino acids (DFG → GFG) that is normally required for coordination of the ATP substrate. As such, kinase activity is at least mostly abolished, but quaternary structure of the receptor is presumably maintained, accounting for the dominant effect. *Velvet* is the first known dominant representative of the *Egfr* allelic series that is fully viable, a fact that makes it particularly useful for developmental studies.

THE mammalian genome is believed to encompass ~30,000–40,000 genes (LANDER *et al.* 2001; VENTER *et al.* 2001), but the number of phenotypes cataloged to date is much smaller than this, and, hence, it may be said that the essential function of most genes remains undetermined (BROWN and PETERS 1996). To close the “phenotype gap,” the chemical mutagen *N*-ethyl-*N*-nitrosourea (ENU) has been widely used to produce random germline mutations in mice (EHLING *et al.* 1985; HRABE DE ANGELIS and BALLING 1998; JUSTICE *et al.* 1999; HRABE DE ANGELIS *et al.* 2000; NOLAN *et al.* 2000; BROWN and BALLING 2001), so that novel phenotypes can be identified, and the mutations responsible for them can be resolved by positional cloning. In this report, we focus on the development of the eyelids in mice, which undergo specific developmental changes both *in utero* and during early postnatal life.

Under normal circumstances, the eyelids begin to grow across the surface of the developing eye at E12.5. Between days 14 and 16 of gestation, the top and bottom eyelids continue to flatten, come to lie in close approximation to one another, and finally fuse tightly with each other at E16.5. They remain fused until ~12 days after birth (FINDLATER *et al.* 1993). Failure of fusion leads to a readily apparent “open-eyelids-at-birth” defect. Eyelid closure is a process involving the migration of epithelial

cells. Mutations that disrupt the signaling interactions between epithelium and the underlying mesenchyme can cause eyelid closure defects. Some examples include recessive mutations in the *Tgfa*, *Egfr*, *MEKK-1*, and *Fgfr2* loci (LUETTEKE *et al.* 1993, 1994; MANN *et al.* 1993; YUJIRI *et al.* 2000; LI *et al.* 2001). A number of unidentified loci, such as *eob*, *Ig<sup>ca</sup>*, *oe*, and *gp* (STEIN *et al.* 1967; JURIOFF *et al.* 2000), can also produce an open-eyelid defect. In some cases, a wavy coat and curly vibrissae accompany open eyelids. This complex of traits is exemplified by the spontaneous mutations *wa-1* and *wa-2*, which represent recessive lesions in the *Tgfa* and *Egfr* genes, respectively.

In the course of a large-scale ENU mutagenesis screening effort carried out in our laboratory, a dominant mutation (*Velvet*) was identified among a total of 16,606 F<sub>1</sub> mice born to mutagenized C57BL/6 males and normal C57BL/6 females. The designation “*Velvet*” refers to the velvet-like texture of the coat of affected animals. However, *Velvet* mice are born with eyelids open and with curled vibrissae as well. They present a phenotype very similar to that of *waved-1* and *waved-2* mice. Although two similar phenotypes (so far unmapped) have been observed among 23,221 F<sub>3</sub> animals generated and weaned to date, *Velvet* was the sole dominant mutation of its type. It quickly became evident that the mutation could not be maintained in the homozygous state (*i.e.*, that it was homozygous lethal). We expanded the phenotype, creating a heterozygous stock, and cloned the mutation positionally.

<sup>1</sup>Corresponding author: Scripps Research Institute, Department of Immunology, IMM-31, 10550 N. Torrey Pines Rd., La Jolla, CA 92037. E-mail: bruce@scripps.edu

## MATERIALS AND METHODS

**Animals:** The C57BL/6J animals used in ENU mutagenesis were purchased from Jackson Laboratories, and C3H/HeN mice used for outcrossing and mapping were purchased from Taconic Farm. All studies involving animals were carried out in accordance with institutional regulations.

**ENU mutagenesis and breeding:** Six-week-old male C57BL/6J mice are treated with ENU administered in three weekly doses (90 mg/kg body weight) by intraperitoneal injection. After 12 weeks of recovery from infertility, each mouse is bred to normal C57BL/6J female mice so as to produce a maximum of 20 offspring. These F<sub>1</sub> animals are either subjected to phenotypic screens or used to produce F<sub>2</sub> mice, which in turn are backcrossed. Two F<sub>2</sub> daughters per sire are backcrossed with the F<sub>1</sub> male to generate F<sub>3</sub> mice. A total of six F<sub>3</sub> females and six F<sub>3</sub> males are produced for screening. Approximately 50% of the mutations carried by each F<sub>1</sub> mouse are transmitted to homozygosity in every panel of six F<sub>3</sub> mice produced according to this scheme. To date, 16,606 F<sub>1</sub> animals and 23,221 F<sub>3</sub> germline mutants have been generated in our laboratory.

**Morphological screening:** All animals are examined for abnormalities affecting the eyes, the color or quality of the coat, development of the limbs or tail, and neurological or behavioral status at birth and at weaning age. All viable F<sub>1</sub> phenodeviants are examined to determine whether the phenotype is heritable. Once transmissibility has been confirmed, each mutation is expanded, bred to homozygosity if possible, and mapped.

**Genomic linkage analysis:** Heterozygotes (first generation) were mated to wild-type C3H/HeN mice; the affected F<sub>1</sub> hybrid mice (second generation) were then crossed with the wild-type C3H/HeN animal again. The offspring of the second generation were phenotyped and tailed for mapping. Genomic DNA was prepared from tail tips with the QIAGEN (Valencia, CA) DNeasy kit and adjusted to a concentration of 50 ng/ $\mu$ l. A total of 59 microsatellite markers were used for genome-wide linkage analysis. After chromosomal linkage was established and low-resolution confinement was achieved, a total of 39 microsatellites were surveyed across the critical region to identify informative markers. A total of 21 novel informative simple sequence length polymorphisms were identified in the *Velvet* region and are shown in Table 1.

**DNA sequencing:** Total RNA was isolated from the liver of a *Velvet* heterozygote on the C57BL/6 background and from a wild-type C57BL/6J mouse, respectively, by the QIAGEN RNeasy mini kit. A total of 1.5  $\mu$ g total RNA was used in RT-PCR to generate cDNA with the RETROscript kit (Ambion, Austin, TX). The coding region of *Egfr* was amplified and directly sequenced to detect mutations. Sequencing was carried out using nested primers on an ABI 3100 sequencer and covered both strands of the template. Contigs were assembled by the programs phred and Phrap, and possible mutations were examined with the aid of the consed and polyphred programs.

**Embryonic studies:** For histological analysis of the eyelids, carriers of the *Velvet* mutation (C57BL/6J background) were bred with normal C57BL/6J mice. The presence of a vaginal plug was taken at 0.5 day of gestation. At E16.5, female animals were euthanized using CO<sub>2</sub> asphyxiation, and embryos were dissected under a dissecting microscope. The heads of affected embryos, which were easily distinguished from those of unaffected embryos, were fixed in 4% paraformaldehyde and embedded in paraffin. Sections were stained with hematoxylin and eosin. The eyelids were examined in transverse section.

To examine the homozygous lethal effect of *Velvet*, heterozygotes (C57BL/6J background) were mated with each other. At specific embryonic stages (E10.5, E11.5, E12.5, E13.5, E15.5,

and E17.5), embryos were dissected free of the uterine wall and subjected to genomic DNA isolation with the QIAGEN DNeasy tissue kit. A total of 100 ng of genomic DNA was used to amplify a 500-bp region that covers the *Egfr* mutation in question. The primers used for PCR were 5' GTCATTCATGC CAGATAATTCCAA 3' and 5' CCAAATGCCATTCACAAAGTA GAG 3'. Genotyping was accomplished by sequencing the PCR products.

To determine whether midgestational defects of the placenta might result in homozygous lethality, heterozygotes (C57BL/6J background) were mated with each other. At E12.5, embryos and corresponding placentas were dissected from the uterine wall. Placentas were fixed in 10% formalin and embedded in paraffin. Sections were stained with hematoxylin and eosin. The embryos were used for genotyping.

**Embryonic fibroblast migration assay:** *Velvet* heterozygotes were mated with wild-type C57BL/6J mice. At E16.5 fetuses were isolated and pooled together by the phenotype. The fetal skin was peeled off and trypsinized at 4° overnight. Cell suspensions were centrifuged at 1200 rpm for 5 min and resuspended in DMEM (Dulbecco's modified eagle medium, GIBCO BRL, Gaithersburg, MD) supplemented with 10% fetal bovine serum. The fifth passage of cells was used for the migration assay.

The cell migration assay was performed using modified Boyden chambers (Transwell; Costar, Cambridge, MA) containing polycarbonate membranes as previously described (KLEMKE *et al.* 1997). The cells were allowed to migrate for 5 hr; the migratory cells attached to the bottom surface of the membrane were stained with 0.1% crystal violet for 20 min at room temperature. The stain was eluted with 10% acetic acid, the absorbance was determined at 590 nm, and the percentage of migratory cells of wild-type or *Velvet* origin was compared.

**In vivo phosphorylation:** Wild-type and *Velvet* heterozygotes (1- to 2-day-old pups) were injected subcutaneously in the neck with phosphate-buffered saline (PBS) or with epidermal growth factor (EGF) dissolved in PBS, at a dose of 10  $\mu$ g/g body weight. Ten minutes later, mice were killed, and their livers were harvested and homogenized in lysis buffer (20 mM Tris, pH 7.5, 150 mM NaCl, 1 mM EDTA, 1 mM EGTA, 1% Triton X-100, 2.5 mM sodium pyrophosphate, 1 mM  $\beta$ -glycerol-phosphate, 1 mM Na<sub>3</sub>VO<sub>4</sub>, 1  $\mu$ g/ml leupeptin, and 1 mM phenylmethylsulfonyl fluoride) as described previously (DONALDSON and COHEN 1992). Homogenates were centrifuged at 14,000  $\times$  g for 5 min, and the protein concentrations in the supernatant were determined with Coomassie plus protein assay (Pierce, Rockford, IL). Equivalent amounts of protein were immunoprecipitated with anti-EGF receptor (EGFR) antibody (Cell Signaling Technology) and protein A-agarose (Sigma, St. Louis) prior to separation by SDS-PAGE using a 10% gel and subsequent immunoblotting. The immunoblot was incubated with anti-EGFR antibody and horseradish peroxidase (HRP)-conjugated secondary antibodies (Cell Signaling Technology) to examine the expression level of EGFR. The protein was detected using the Phototope-HRP chemiluminescent detection system (Cell Signaling Technology). The blot was subsequently stripped and reprobed with anti-phosphotyrosine antibody (Cell Signaling Technology) to evaluate the autophosphorylation level of EGFR. The signals were measured using a personal densitometer (Molecular Dynamics, Sunnyvale, CA).

***Egfr*<sup>Velvet</sup> expression construct and transfection of HEK293 cells:** The cDNA of *Egfr*<sup>Velvet</sup> with internal signal sequence removed was amplified using primers 5' CCCAAGCTTTTGGAG GAAAAGAAAGTCTGC 3' and 5' GGAAGATCTTCATGCTCC AATAAACTCGCTGCT 3'. The cDNA was then cloned into pFLAG-CMV-3 expression vector (Sigma) between *Hind*III and *Bgl*III sites. The construct was verified by DNA sequencing.

TABLE 1  
Informative microsatellite markers identified in the *Velvet* region on chromosome 11

Marker	Primers (F/R)	Distance from centromere (bp) <sup>a</sup>	Length (bp)	
			C57BL/6	C3H/HeN
Vel_1	5' AACCAGACATTAGCATCAGCACCTCC 3'	11,604,961	213	200
	5' CACTCTTTCCAGCGCTATTTAGGTATGG 3'	11,605,170		
Vel_3	5' AAGAGGCAGGTTGTTCCACTTATTACCCAG 3'	11,735,361	174	215
	5' GCTGCTCTGCTTCTCTTGATAATTTCC 3'	11,735,530		
Vel_5	5' TGTGCATGAATGTGCTTATGTGTTTATGTG 3'	11,888,469	129	140
	5' ACACCAAGGATGTTTGTGATTTACAGCC 3'	11,888,590		
Vel_6	5' ACATGTCCAGATGGTAAGGGAAGACAATC 3'	11,902,211	258	234
	5' TGCACGTCTGCTTGTGTGACTGTAATTC 3'	11,902,464		
Vel_8	5' GGTGATAAATCCATGGGATTTGATTGC 3'	10,901,453	279	257
	5' GCAAGCTGACACATGGTGTGTGAGTACCTTAG 3'	10,901,727		
Vel_9	5' TGGAAGTGACTTACCTGAAAGGAGCAG 3'	11,038,963	278	246
	5' GCATGCCTCTGTTCTTGTCTCAGTGTAC 3'	11,039,237		
Vel_10	5' CACGCATCTTGTAATTCAGAAATATCATTTTC 3'	11,354,992	175	168
	5' ACATCTGCTCTAGTTTCAAAAGTGCTGG 3'	11,355,162		
Vel_12	5' CATAGGCTGCCATTTGCTTTCTAGACTAAG 3'	11,546,860	272	263
	5' GGTGTGACTCGTACTATTCCCTCAACTCTTC 3'	11,547,121		
Vel_13	5' TGTCCCTCACATCAGAAGCCATTACTATAAG 3'	11,897,142	219	215
	5' CCTCCTAACCAATTGTAACACTTCCACTATG 3'	11,897,364		
Vel_14	5' GCCATATTGAGCAACACCATGTATATCTTG 3'	12,383,221	317	308
	5' CCTCAGTCAACTGATGTTGCAAGGTAATC 3'	12,383,533		
Vel_18	5' GAAAGCTTGGTAGTGTCTAATGGGAAGAAC 3'	13,078,774	300	302
	5' GCTTTCTTCTTGACATTCAGTTCCG 3'	13,079,066		
Vel_19	5' TGCTTCCATAAGAAATTCAGACCATCTATC 3'	13,090,106	159	163
	5' CAGATGTGATTGGCTAGGCAAGATAATGAAG 3'	13,090,256		
Vel_23	5' TCTATAGGTGGCCATGATTGTAAGAAGTGAG 3'	12,619,246	157	154
	5' AGATGTGGAAGTAAAGGGAGTTTGTATGATG 3'	12,619,397		
Vel_26	5' GCCTCCAGAGTGGTCTACACGATG 3'	13,541,828	170	157
	5' GCTGGAGTAACATTAAGCTGCTAGTGAAGAG 3'	13,541,993		
Vel_27	5' GGAACAAGCTCTGTCAGAAATCTGGC 3'	13,542,524	117	115
	5' TCATCAGGCAAGGCAGAGCTAATTTTC 3'	13,542,638		
Vel_29	5' AGCTTCCCTTTGTGCTGGTGAATCATTATAG 3'	13,678,867	178	176
	5' TCCAGAGTATAGTTGCAAACCAGTGGC 3'	13,679,036		
Vel_30	5' CAGGATGAAAGTAGTGTGTATGCATGTG 3'	13,712,758	192	198
	5' ATAGAACTAACATACCAGGAGAAAGCCCTTTC 3'	13,712,942		
Vel_31	5' CTACCTGAGTGTGTCCATGTGTATGGTATATG 3'	13,726,855	133	139
	5' GGCTGTGGCACTGATAATGCTTGC 3'	13,726,980		
Vel_35	5' GGGAAAGGAAGATTGTATCTGAGGGTTG 3'	13,967,121	240	247
	5' GCTTTCATTCTTCTGTATATTCTGCTCCTGG 3'	13,967,354		
Vel_36	5' GCCTCAGCCCTGAAAAATACATACAAG 3'	14,061,338	219	207
	5' TCTTAAACCTCATATAAACCCCAATAAGG 3'	14,061,548		
Vel_37	5' CTCGAAATATTGATGTGTAGCCTCTTGTG 3'	14,070,899	302	311
	5' GTTGACAGAGACATAAGACTTCAAAGTGACC 3'	14,071,193		

<sup>a</sup> The distance is deduced from the Celera database.

HEK293 cells were purchased from the American Type Culture Collection and grown in DMEM (GIBCO BRL) supplemented with 10% FBS, 2% penicillin/streptomycin. Cells were transfected with either pFLAG-CMV-3 vector or *Egfr*<sup>Velvet</sup> expression construct (amount indicated) using Fugene 6 (Roche). The cellular response to EGF stimulation was tested 48 hr posttransfection. At that time, transfected cells were serum starved for 24 hr and then stimulated with EGF (1 nM final concentration) for 10 min at 37°. Then whole cell lysates (12 µg/lane of protein) were subjected to Western blotting using antibodies against *phospho*-mitogen-activated protein kinase (*phospho*-MAPK), MAPK, and a Flag epitope.

**Immunoblotting of activated MAPK:** Transfected 293 cells were serum starved for 24 hr before being stimulated with 1 nM EGF for 10 min at 37°. Cells were rinsed twice with PBS, lysed in lysis buffer, scraped from the plates, transferred into a microcentrifuge tube, and kept on ice. Samples were sonicated for 5 sec four times to shear genomic DNA and reduce viscosity. The lysate was clarified by centrifugation at 14,000 rpm for 10 min, and the amount of total protein was determined with Coomassie plus protein assay (Pierce). Equivalent amounts of protein were separated by a 10% SDS-PAGE gel and transferred to nitrocellulose membrane. The activation of MAPK was monitored by Western blotting using antibodies

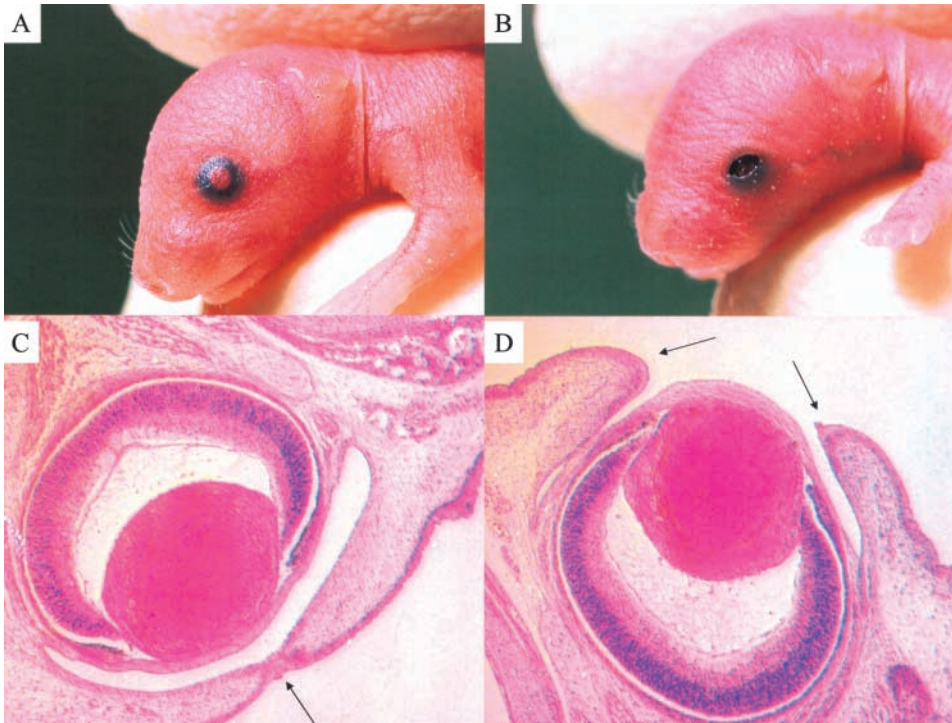


FIGURE 1.—Failure of eyelid closure in *Velvet* mice. (A and C) Wild-type mice; (B and D) *V/+* heterozygotes. Neonatal *Velvet* mice are born with eyelids open (B), whereas the eyelids of wild-type littermates remain closed until 12 days after birth (A). The upper and lower eyelids of a normal embryo are fused in the midline at E16.5 (arrow), whereas the eyelids of a *Velvet* embryo remain apart (C and D). Embryos were fixed in 4% paraformaldehyde and embedded in paraffin, cut in transverse section, and stained with hematoxylin and eosin.

against the phosphorylated form of MAPK (Cell Signaling Technology). The amount of total endogenous MAPK loaded for each sample was verified by probing against MAPK with a nonphosphospecific antibody.

## RESULTS

*Velvet* was identified in  $F_1$  mice born to an ENU-treated sire and was assumed to be a dominant mutation. The phenotype proved to be readily transmissible. Analysis of the transmission ratio, determined by counting the number of normal and *Velvet* pups on a hybrid background (C57BL/6J *Velvet*  $\times$  C3H/HeN), was consistent

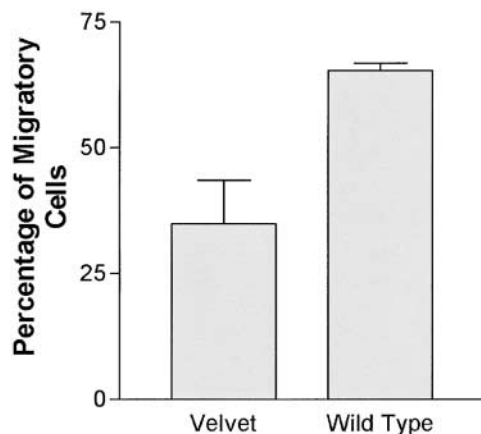


FIGURE 2.—Embryonic fibroblast migration assay. Cells from *Velvet* embryos showed defective migration ability. The result was based on two individual experiments. Error bars indicate standard deviation.

with the conclusion that *Velvet* heterozygotes are fully viable to term. Among 360 animals produced in such crosses, 184 showed the *Velvet* phenotype. Hence, it also appears that the mutation is fully penetrant.

Heterozygous *Velvet* mice are born with eyelids open and with curly vibrissae. Their first coat is wavy; later, the pelage hair loses its wavy appearance and becomes disoriented, with individual shafts projecting in various directions relative to neighboring shafts. The eyes of adult *Velvet* mice are often small, with corneal opacity, and excessive secretions are always seen at the edges of eyelids. Aside from the eyelid and fur abnormalities, heterozygous animals appear healthy and show normal fertility. Compared to their littermates, *Velvet* mice have a normal body size and exhibit normal cage activities.

The eyelid defect as it appears in neonatal *Velvet* mice is depicted in Figure 1. As seen in histological sections (Figure 1, C and D), the upper and lower eyelids of normal mice become approximated and then fuse to a state of closure by E16.5, whereas the eyelids of *Velvet* embryos remain far apart, never coming into contact with one another. The protruding ridges of *Velvet* eyelids were well formed, and growth across the cornea seemed to be initiated in the presence of the mutation as well, but migration of epithelia cells was defective compared to that in normal mice.

Migration of eyelid epithelial cells is difficult to quantify *in vivo*. To provide a numerical index of the migration defect, and to demonstrate that the mutation imparted a cellular phenotype *in vitro*, we analyzed the migration of embryonic fibroblasts isolated from wild-type and *Velvet* embryos. The fibroblasts from *Velvet* em-

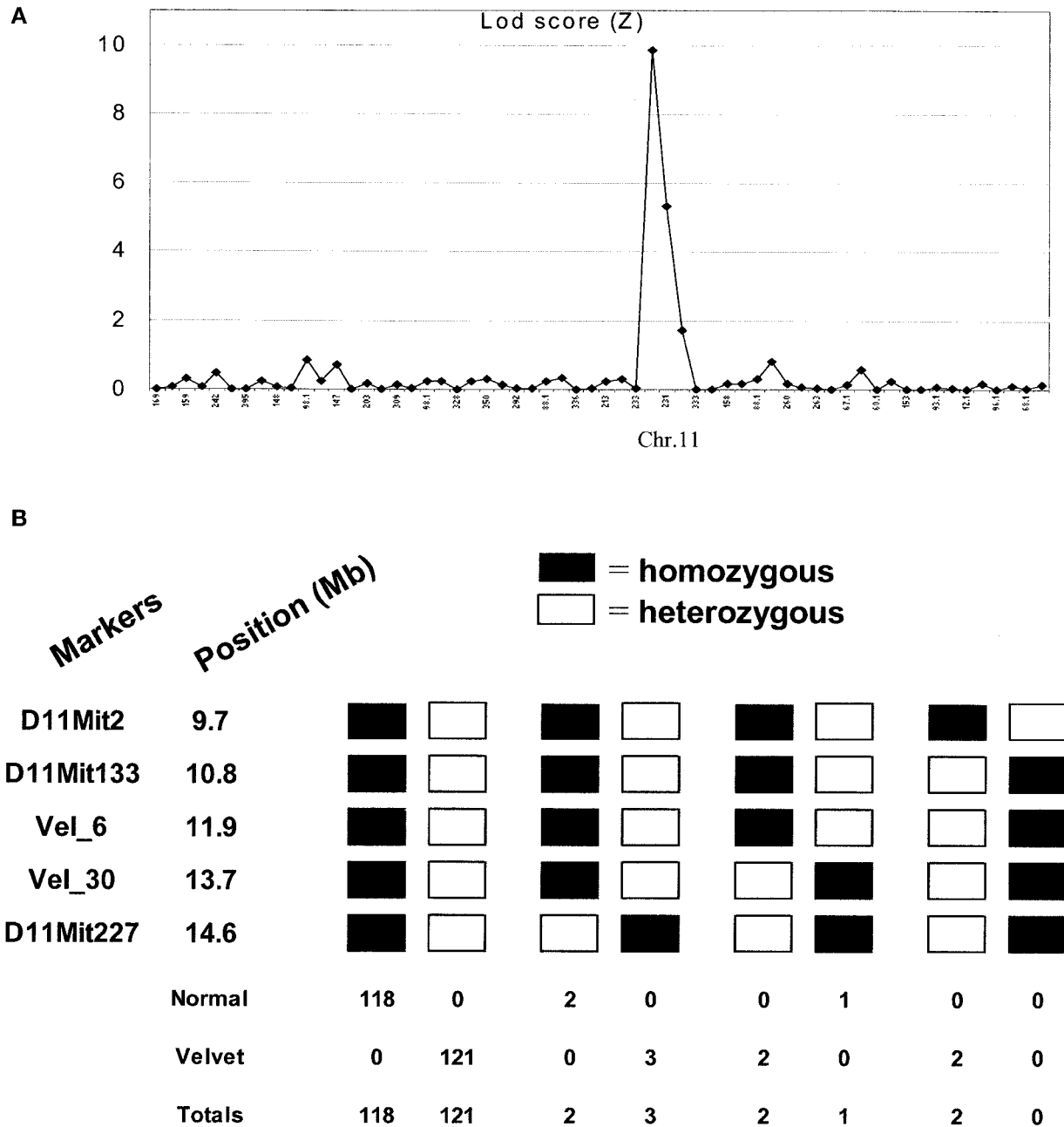


FIGURE 3.—Genetic mapping of the *Velvet* locus. (A) Whole-genome linkage analysis. On 51 meioses, the *Velvet* locus is confined to the proximal end of chromosome 11 with a peak LOD score of 9.8. A total of 59 microsatellite markers were used. (B) Fine genetic mapping of the *Velvet* locus. On 249 meioses, the mutation is confined within the region flanked by markers *Vel\_6* and *D11Mit227*. There are three crossovers on the proximal side and five crossovers on the distal end. The position of markers is presented with reference to the Celera database.

bryos demonstrate ~53% of the migratory ability of wild-type embryos (Figure 2).

Aside from the eyelid defect, other structures of the eye seem normal. Since the open eyelids constantly leave the cornea exposed, the corneal opacity and excess secretion displayed by adult *Velvet* mice might not be due to developmental defects, but rather to infection, drying, and possibly trauma.

By analyzing 249 meioses, we were able to confine the

*Velvet* mutation to an interval 3.2 cM in length, demarcated by the microsatellite markers *Vel\_6* and *D11Mit227*. The critical regions lie near the proximal end of chromosome 11, occupying a 2.7-Mb interval (11.9–14.6 Mb from the centromere; Celera distances; Figure 3). Within the critical region, 38 annotated genes are listed in the Celera database. Ten of these are pseudogenes and 28 are authentic genes. Among the authentic genes, *Egfr* was considered the most promising candi-

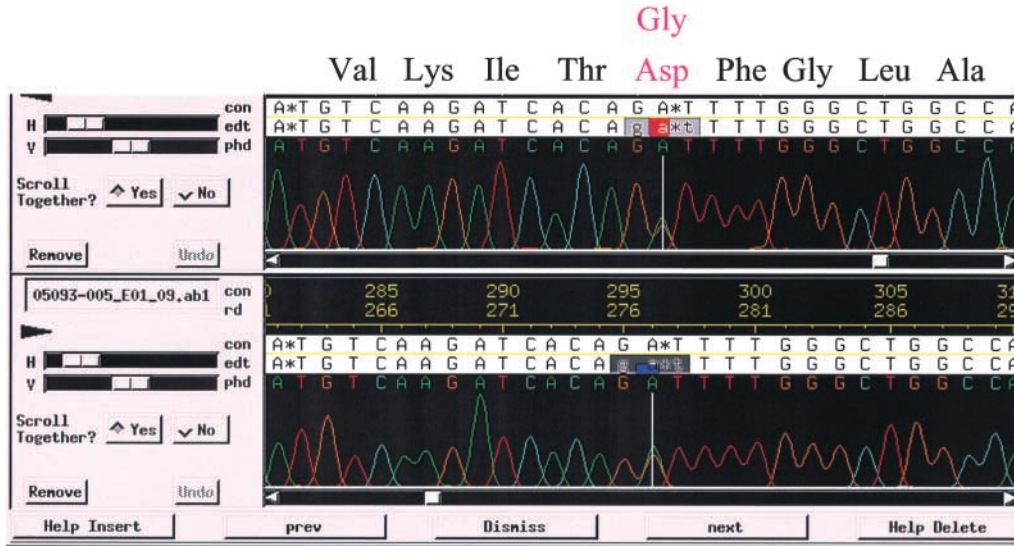


FIGURE 4.—*Velvet* corresponds to a single-base-pair substitution of the *Egfr* gene. This A → G transition results in Asp replacement by Gly. The consed display shows bidirectional sequencing of the heterozygous *Egfr* mutation using a template amplified from a mouse with the *Velvet* phenotype.

date, given the fact that the *wa-2* phenotype (very similar to the *Velvet* phenotype) was caused by a spontaneous recessive mutation in *Egfr* (LUETTEKE *et al.* 1994). The EGF receptor is expressed in a wide range of adult tissues and cell types (PARIA and DEY 1990), and it is believed that activation of the EGF receptor signaling pathway contributes to the regulation of numerous cellular processes, both during embryonic development and in the adult (CARPENTER and COHEN 1990; WELLS 1999).

The complete coding region of *Egfr* was amplified from liver cDNA, prepared from normal C57BL/6 mice and *Velvet* heterozygotes, respectively. A single heterozygous nucleotide substitution was detected in the *Velvet* template (Figure 4). This, an A → G transition, typical of ENU mutations (JUSTICE *et al.* 1999), is predicted to cause the replacement of an aspartic acid residue at position 833 with a glycine. The mutation thereby alters the structure of the EGF receptor cytoplasmic tyrosine kinase domain and falls within a triad of residues—the DFG motif—known to be important for ATP coordination (STAMOS *et al.* 2002).

Previous work has revealed that injection of EGF into a newborn mouse can rapidly induce EGFR tyrosine phosphorylation (DONALDSON and COHEN 1992), which occurs through an internal autophosphorylation mechanism (HUBBARD *et al.* 1998). To examine *Velvet* EGFR activity *in vivo*, neonatal *Velvet* mice and their wild-type littermates were injected subcutaneously, either with PBS alone or with EGF dissolved in PBS. As expected, in the wild-type mouse, injection of EGF led to enhanced tyrosine phosphorylation of EGFR. In the *Velvet* heterozygote, there was a sixfold decrease of EGFR autophosphorylation after EGF challenge as compared with the wild-type control. Moreover, basal tyrosine phosphorylation of EGFR was reduced by threefold (Figure 5).

The dominant effect of *Egfr<sup>Velvet</sup>* was observed *in vitro* as well (Figure 6). Human epithelial cell line 293 cells,

known to express EGFR and ErbB2 protein (data not shown), were transiently transfected either with various amounts of an *Egfr<sup>Velvet</sup>* expression construct or with empty vector as a control. Upon 1 nM EGF stimulation, cells transfected with empty expression vector showed pronounced induction of the activated form of MAPK (*phospho*-MAPK, p42/p44); the *Egfr<sup>Velvet</sup>* expression construct caused a dose-dependent inhibitory effect on MAPK activation.

Because *Velvet* homozygotes were never observed at term throughout the course of our studies, we considered the mutation to be homozygous lethal. We wished to determine the stage at which death occurs *in utero*. We therefore intercrossed *Velvet* heterozygotes (C57BL/6 back-

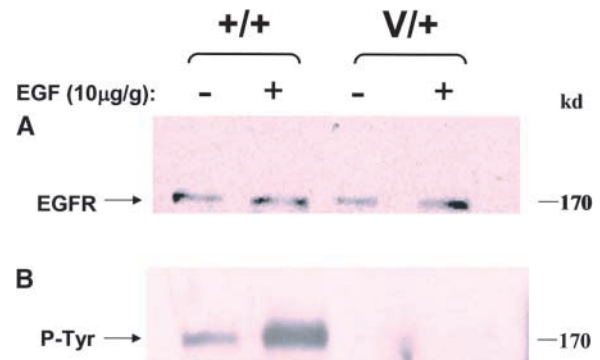


FIGURE 5.—EGF-induced autophosphorylation of EGFR *in vivo*. (A) EGFR expression in liver dissected from a neonatal *Velvet* mouse (*V/+* genotype) and a wild-type littermate, respectively. Two-day-old pups were injected with PBS or with EGF in PBS (10 µg/g body weight) subcutaneously in the neck. Ten minutes later, pups were killed and livers were removed and homogenized. Equivalent amounts of protein were subjected to immunoprecipitation and subsequent immunoblotting with anti-EGFR antibody. (B) Tyrosine phosphorylation of EGFR upon EGF stimulation. Immunoblot from A was stripped and reprobed with anti-phosphotyrosine antibody.

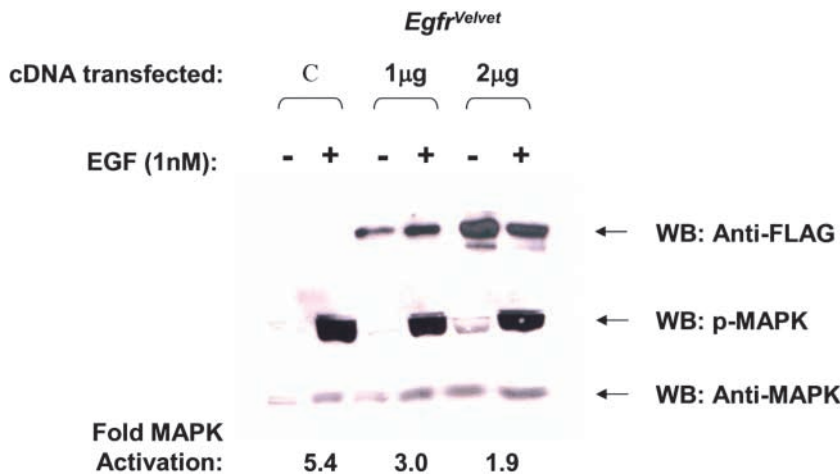


FIGURE 6.—EGF-induced activation of MAPK *in vitro*. A total of 293 cells were transfected with either 2 µg of empty pFLAG-CMV-3 vector (C) or pFLAG-CMV-3 containing the *Egfr<sup>Velvet</sup>* expression construct (amounts indicated). The level of MAPK activation was normalized to take account of the total amount of endogenous MAPK loaded per lane.

ground) to determine whether homozygosity for *Velvet* was compatible with survival to a postembryonic stage of development (Table 2). Dividing gestation into windows of time, we observed that between E10.5 and E11.5, the genotypic distribution (+/+:+/V:V/V) was 5:9:3. Between E12.5 and E13.5, the distribution was 5:13:2. Between E15.5 and E17.5 the distribution was 5:18:0. And at term, the distribution was 11:17:0. These data (along with phenotypic assessments of a much larger number of mice, mentioned earlier) suggest that heterozygotes have no diminution in viability. However, homozygotes show a trend toward diminished viability during embryonic life and die between E13.5 and E15.5, a time that roughly corresponds to the transition between embryonic and postembryonic life (E14.5).

Histological analysis of E12.5 placentas revealed that the labyrinth trophoblast layer in homozygous placenta was disorganized. The cell number was greatly reduced when compared to the placenta of wild-type and heterozygous embryos, and a number of dead or dying cells were evident. The organization and cell number of the giant-cell layer of the trophoblast were fairly normal (Figure 7). Since fetal nutrition depends on the placental labyrinthine layer, we consider it likely that homozy-

gosity for *Egfr<sup>Velvet</sup>* produces midgestation lethality due to a placental defect.

## DISCUSSION

*Velvet* is a new member of the *Egfr* allelic series. Although an EGFR construct with at least some dominant negative properties has been expressed in mice as the product of a transgene (MURILLAS *et al.* 1995), no *in situ* modification of the *Egfr* locus has previously been shown to yield a dominant effect. Hence, *Velvet* is the sole dominant representative of the *Egfr* allelic series described to date. It results from a point mutation within exon 21 (of 28 exons in the gene) that causes an amino acid substitution (D833G) within a highly conserved motif of the receptor tyrosine kinase domain.

From the crystal structure of the EGF receptor tyrosine kinase domain, D<sup>833</sup> lies within the “DFG motif,” which defines the beginning of the “activation loop” and is important for ATP coordination (STAMOS *et al.* 2002). This residue (and the whole of the DFG motif, as well as several flanking amino acids) is strictly conserved in all known EGF receptor sequences from a broad range of species. Moreover, in PRINTS (a protein fingerprint database; <http://www.bioinf.man.ac.uk>), it is observed that the DFG motif is invariably found as a part of the tyrosine kinase catalytic domain signature. The inflexibility of the DFG motif suggests its conformational importance: by interacting with other residues, the DFG motif is believed to provide a favorable structural arrangement for the “catalytic loop” to accommodate the ATP binding. At the same time, the DFG motif may help the activation loop attain or stabilize the conformation required for catalytic activity upon phosphorylation (HUBBARD *et al.* 1998; STAMOS *et al.* 2002). The D833G mutation replaces the relatively large, acidic side chain with a hydrogen atom. The steric and/or charge effect of the mutation is evidently sufficient to adversely affect receptor function and to do so in a dominant fashion. *In vivo*, although EGFR is clearly expressed,

TABLE 2

### Embryonic lethality in *Velvet* homozygotes

Days	+/+ (%)	+/V <sup>a</sup> (%)	V/V <sup>a</sup> (%)
E10.5	1 (25)	2 (50)	1 (25)
E11.5	4 (30.8)	7 (53.8)	2 (15.4)
E12.5	4 (33.3)	7 (58.3)	1 (8.3)
E13.5	1 (12.5)	6 (75)	1 (12.5)
E15.5 <sup>b</sup>	3 (17.6)	14 (82.4)	0
E17.5 <sup>b</sup>	2 (33.3)	4 (66.7)	0
Newborn	11 (39.3)	17 (60.7)	0

<sup>a</sup> V, *Velvet*.

<sup>b</sup> Dead embryos observed at E15.5 and E17.5 were found to be of the V/V genotype, but only living embryos are listed.

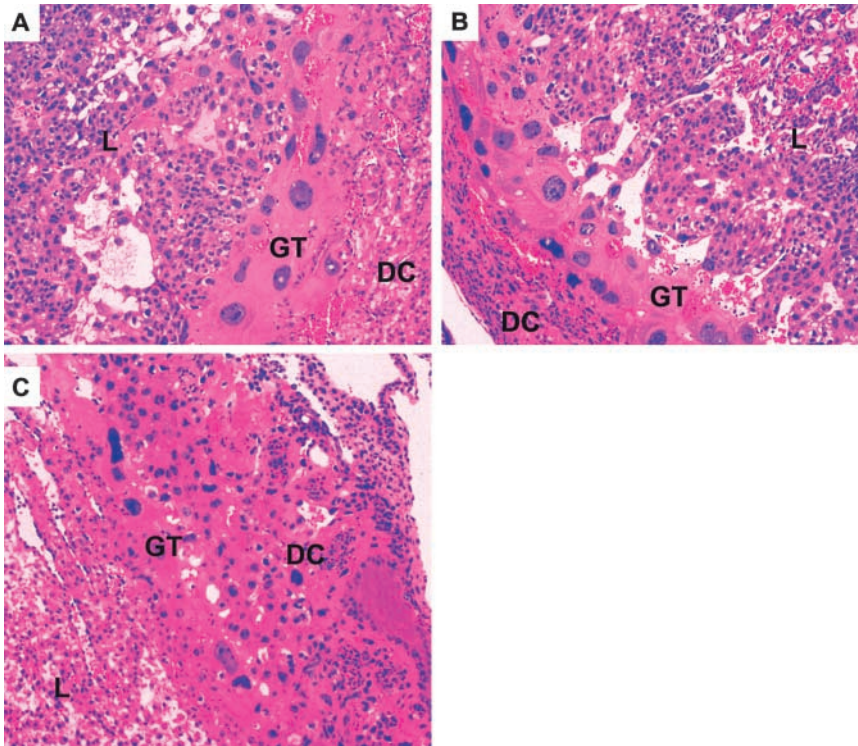


FIGURE 7.—Histologic analysis of mid-gestation placentas. E12.5 placentas were sectioned and stained with hematoxylin and eosin. The genotypes were determined by PCR amplification of genomic DNA from the corresponding embryos. (A) Wild type; (B) *V/+*; (C) *V/V*. DC, decidua; GT, trophoblast giant cells; L, labyrinthine placenta.

inducible autophosphorylation occurred at only one-sixth the level observed in a wild-type littermate. In this respect, the phenotypic effect of the *Velvet* mutation is distinguishable from that of a null allele, which is strictly recessive.

The outer root sheath of the hair follicle and the epidermal layer of the eyelid probably express EGFR in greater abundance than do most other tissues (GREEN *et al.* 1983; MURILLAS *et al.* 1995) and, on this basis, may be markedly dependent upon EGFR, a circumstance that may make them particularly sensitive to perturbations in EGFR signal transduction. Targeted expression of a truncated human EGFR (HERCD-533, which has proved to act as a dominant negative mutant) to the basal layer of epidermis and outer root sheath of hair follicles of transgenic mice severely alters hair follicle development and skin structure. Most of these mice eventually developed alopecia (MURILLAS *et al.* 1995). Both the outer root sheath of the hair follicle and the epidermal layer of the eyelid display an immense proliferative capacity and probably depend upon EGFR as a regulator of cell migration through the extracellular matrix, a process that is highly dependent upon interactions between epithelium and underlying mesenchyme. Upon binding its ligands (mainly TGF- $\alpha$  and EGF), EGFR activates multiple signaling pathways to stimulate epithelial cell proliferation and migration (JHAPPAN *et al.* 1990; SANDGREN *et al.* 1990; WILSON and GIBSON 1999). EGFR is linked to two pathways of particular importance in the promotion of cell motility: the phospholipase C $\gamma$  (PLC $\gamma$ )-protein kinase C (PKC) and the

Ras-MAPK pathways. Once activated, PLC $\gamma$  catalyzes the hydrolysis of phosphatidylinositol (4,5)-bisphosphate to yield the second messengers diacylglycerol and inositol-1,4,5-triphosphate, which effect calcium release from intracellular stores and activate the PKC-mediated cascade (WELLS 1999; JORISSEN *et al.* 2003). At the same time, EGFR activation induces immediate activation of the Ras/MAPK pathway, which can enhance myosin light chain kinase (MLCK) activity, leading to phosphorylation of myosin light chains (MLC; KLEMKE *et al.* 1997). Thus, through the PLC $\gamma$  and Ras/MAPK signaling cascade, EGFR directly influences the motility machinery of the cell. These two signaling pathways are not only activated simultaneously but also interlinked with each other, presenting a complex but delicate regulatory system. Any mutation that disrupts signal transduction in these pathways will cause dysregulation of cell migration. This effect is likely manifested in defects of eyelid and hair development, as seen in mice with the *wa-1*, *wa-2*, *MEKK1*, and *Velvet* mutations.

Depending upon their genetic background, *Egfr*<sup>-/-</sup> mice die during the peri-implantation stage due to degeneration of the inner cell mass or during mid-gestation as a result of placental defects or are born with their eyes open but live only up to 3 weeks of postnatal life as a result of respiratory problems, epithelial immaturity, and multiorgan abnormalities (SIBILIA and WAGNER 1995; THREADGILL *et al.* 1995; MIETTINEN *et al.* 1999), while the *Velvet* heterozygotes show abnormalities in only the eyelids and hair follicles. On the other hand, *Velvet* homozygotes die in late embryonic life due to the placental

insufficiency, whether the mutation is on the C57BL/6 background or on a mixed C3H/HeN × C57BL/6 background. The strong dominant effect of the *Velvet* allele may have two general explanations, neither of which excludes the other.

First, it is believed that EGFR activation involves the formation of an active homodimer upon ligand binding, and the activation is achieved by autophosphorylation that occurs in a “*trans*” mode in the receptor complex. Since normal levels of EGFR expression are observed in *Velvet* heterozygotes, it is likely that the integrity of dimer formation is undisturbed by the mutation; however, EGF signaling clearly is interrupted, consistent with the loss of three-quarters of receptor activity (to be expected with a kinase-dead dominant subunit residing in a dimeric protein) or perhaps even more.

Second, the interaction between EGFR and other cell surface protein kinases of the ErbB family leads to the formation of heterodimers or even hetero-oligomers. For example, ErbB2 is the preferred heteromeric partner for EGFR (YARDEN and SLIWKOWSKI 2001; SCHLESINGER 2002; JORISSEN *et al.* 2003). While the ligand for the ErbB2 heteromer is presently unknown, the biological activity of ErbB2 is at least largely dependent upon the formation of a heterodimer or hetero-oligomer with EGFR. The product of the *Velvet* allele might potentially disrupt signal transduction through EGFR homodimers and EGFR/ErbB2 heteromers alike, as well as transduction through other receptor complexes. In this respect, a kinase-dead allele would predictably be more deleterious than a null allele.

*In vitro*, the inhibitory effect of the *Egfr*<sup>*Velvet*</sup> product on the EGF-induced MAPK activation was readily demonstrated, confirming that the mutant allele is capable of disrupting the function of the normal allele. Inhibition was dose dependent and consistent with the poison subunit model proposed.

We further note that homozygosity for the *wa2* allele creates a phenotype approximately similar to that of heterozygosity for *Velvet*. Overall, we suggest that phenotypic severity of different genotypes might be graded as follows:

$$\underline{V/V} > \underline{V/-} > \underline{V/wa2} > \underline{-/-} \gg \underline{V/+} \approx \underline{wa2/wa2} > \underline{-/+} \approx \underline{wa2/+} \approx \underline{+/+}.$$

Not all genotypic components of the series (those that are not underlined) have yet been examined, and, in particular, the phenotypic effect of compound heterozygosity for *Velvet* and either the *wa2* or null allele (not underlined above) remains a matter of speculation.

The fact that a heterozygous animal is morphologically marked and fully viable while homozygosity is embryonic lethal may make the *Velvet* mutation particularly useful for developmental studies. Moreover, differences between the phenotype of *Velvet* and the phenotype of other *Egfr* alleles may permit added insight into the role played by specific components of the EGFR/ErbB receptor family.

The authors are grateful for the assistance of Adrian Smith in the histologic analysis of embryonic placentas. This work was supported by funding from National Institutes of Health grants GM067759, GM60031, U54AI54523, and 2P01-AI40682 and by a grant from the Defense Advanced Research Projects Agency.

*Note added in proof:* We have become aware of an independent dominant hypomorphic allele of *Egfr*, reported by C. THAUNG, K. WEST, B. J. CLARK, L. MCKIE, J. E. MORGAN *et al.* (2002, Novel ENU-induced eye mutations in the mouse: models for human eye disease. *Hum. Mol. Genet.* **11**: 755–767). The molecular defect responsible for this allele, *Wa*<sup>5</sup>, has not yet been reported.

#### LITERATURE CITED

- BROWN, S. D., and R. BALLING, 2001 Systematic approaches to mouse mutagenesis. *Curr. Opin. Genet. Dev.* **11**: 268–273.
- BROWN, S. D., and J. PETERS, 1996 Combining mutagenesis and genomics in the mouse—closing the phenotype gap. *Trends Genet.* **12**: 433–435.
- CARPENTER, G., and S. COHEN, 1990 Epidermal growth factor. *J. Biol. Chem.* **265**: 7709–7712.
- DONALDSON, R. W., and S. COHEN, 1992 Epidermal growth factor stimulates tyrosine phosphorylation in the neonatal mouse: association of a M(r) 55,000 substrate with the receptor. *Proc. Natl. Acad. Sci. USA* **89**: 8477–8481.
- EHLING, U. H., D. J. CHARLES, J. FAVOR, J. GRAW, J. KRATOCHVILOVA *et al.*, 1985 Induction of gene mutations in mice: the multiple endpoint approach. *Mutat. Res.* **150**: 393–401.
- FINDLATER, G. S., R. D. MCDUGALL and M. H. KAUFMAN, 1993 Eyelid development, fusion and subsequent reopening in the mouse. *J. Anat.* **183** (1): 121–129.
- GREEN, M. R., D. A. BASKETTER, J. R. COUCHMAN and D. A. REES, 1983 Distribution and number of epidermal growth factor receptors in skin is related to epithelial cell growth. *Dev. Biol.* **100**: 506–512.
- HRABE DE ANGELIS, M., and R. BALLING, 1998 Large scale ENU screens in the mouse: genetics meets genomics. *Mutat. Res.* **400**: 25–32.
- HRABE DE ANGELIS, M. H., H. FLASWINKEL, H. FUCHS, B. RATHKOLB, D. SOEWARTO *et al.*, 2000 Genome-wide, large-scale production of mutant mice by ENU mutagenesis. *Nat. Genet.* **25**: 444–447.
- HUBBARD, S. R., M. MOHAMMADI and J. SCHLESINGER, 1998 Auto-regulatory mechanisms in protein-tyrosine kinases. *J. Biol. Chem.* **273**: 11987–11990.
- JHAPPAN, C., C. STAHL, R. N. HARKINS, N. FAUSTO, G. H. SMITH *et al.*, 1990 TGF alpha overexpression in transgenic mice induces liver neoplasia and abnormal development of the mammary gland and pancreas. *Cell* **61**: 1137–1146.
- JORISSEN, R. N., F. WALKER, N. POULIOT, T. P. GARRETT, C. W. WARD *et al.*, 2003 Epidermal growth factor receptor: mechanisms of activation and signalling. *Exp. Cell Res.* **284**: 31–53.
- JURILOFF, D. M., M. J. HARRIS, K. G. BANKS and D. G. MAH, 2000 Gaping lids, gp, a mutation on centromeric chromosome 11 that causes defective eyelid development in mice. *Mamm. Genome* **11**: 440–447.
- JUSTICE, M. J., J. K. NOVEROSKE, J. S. WEBER, B. ZHENG and A. BRADLEY, 1999 Mouse ENU mutagenesis. *Hum. Mol. Genet.* **8**: 1955–1963.
- KLEMKE, R. L., S. CAI, A. L. GIANNINI, P. J. GALLAGHER, P. DE LANEROLLE *et al.*, 1997 Regulation of cell motility by mitogen-activated protein kinase. *J. Cell Biol.* **137**: 481–492.
- LANDER, E. S., L. M. LINTON, B. BIRREN, C. NUSBAUM, M. C. ZODY *et al.*, 2001 Initial sequencing and analysis of the human genome. *Nature* **409**: 860–921.
- LI, C., H. GUO, X. XU, W. WEINBERG and C. X. DENG, 2001 Fibroblast growth factor receptor 2 (Fgfr2) plays an important role in eyelid and skin formation and patterning. *Dev. Dyn.* **222**: 471–483.
- LUETTEKE, N. C., T. H. QIU, R. L. PEIFFER, P. OLIVER, O. SMITHIES *et al.*, 1993 TGF alpha deficiency results in hair follicle and eye abnormalities in targeted and waved-1 mice. *Cell* **73**: 263–278.
- LUETTEKE, N. C., H. K. PHILLIPS, T. H. QIU, N. G. COPELAND, H. S. EARP *et al.*, 1994 The mouse waved-2 phenotype results from a

- point mutation in the EGF receptor tyrosine kinase. *Genes Dev.* **8**: 399–413.
- MANN, G. B., K. J. FOWLER, A. GABRIEL, E. C. NICE, R. L. WILLIAMS *et al.*, 1993 Mice with a null mutation of the TGF alpha gene have abnormal skin architecture, wavy hair, and curly whiskers and often develop corneal inflammation. *Cell* **73**: 249–261.
- MIETTINEN, P. J., J. R. CHIN, L. SHUM, H. C. SLAVKIN, C. F. SHULER *et al.*, 1999 Epidermal growth factor receptor function is necessary for normal craniofacial development and palate closure. *Nat. Genet.* **22**: 69–73.
- MURILLAS, R., F. LARCHER, C. J. CONTI, M. SANTOS, A. ULLRICH *et al.*, 1995 Expression of a dominant negative mutant of epidermal growth factor receptor in the epidermis of transgenic mice elicits striking alterations in hair follicle development and skin structure. *EMBO J.* **14**: 5216–5223.
- NOLAN, P. M., J. PETERS, M. STRIVENS, D. ROGERS, J. HAGAN *et al.*, 2000 A systematic, genome-wide, phenotype-driven mutagenesis programme for gene function studies in the mouse. *Nat. Genet.* **25**: 440–443.
- PARIA, B. C., and S. K. DEY, 1990 Preimplantation embryo development in vitro: cooperative interactions among embryos and role of growth factors. *Proc. Natl. Acad. Sci. USA* **87**: 4756–4760.
- SANDGREN, E. P., N. C. LUETTEKE, R. D. PALMITER, R. L. BRINSTER and D. C. LEE, 1990 Overexpression of TGF alpha in transgenic mice: induction of epithelial hyperplasia, pancreatic metaplasia, and carcinoma of the breast. *Cell* **61**: 1121–1135.
- SCHLESSINGER, J., 2002 Ligand-induced, receptor-mediated dimerization and activation of EGF receptor. *Cell* **110**: 669–672.
- SIBILIA, M., and E. F. WAGNER, 1995 Strain-dependent epithelial defects in mice lacking the EGF receptor. *Science* **269**: 234–238.
- STAMOS, J., M. X. SLIWKOWSKI and C. EIGENBROT, 2002 Structure of the epidermal growth factor receptor kinase domain alone and in complex with a 4-anilinoquinazoline inhibitor. *J. Biol. Chem.* **277**: 46265–46272.
- STEIN, K. F., B. E. NORRIS and J. MASON, 1967 Development of an open eyelid mutant in *mus musculus*. *Dev. Biol.* **16**: 315–330.
- THREADGILL, D. W., A. A. DLUGOSZ, L. A. HANSEN, T. TENNENBAUM, U. LICHTI *et al.*, 1995 Targeted disruption of mouse EGF receptor: effect of genetic background on mutant phenotype. *Science* **269**: 230–234.
- VENTER, J. C., M. D. ADAMS, E. W. MYERS, P. W. LI, R. J. MURAL *et al.*, 2001 The sequence of the human genome. *Science* **291**: 1304–1351.
- WELLS, A., 1999 EGF receptor. *Int. J. Biochem. Cell Biol.* **31**: 637–643.
- WILSON, A. J., and P. R. GIBSON, 1999 Role of epidermal growth factor receptor in basal and stimulated colonic epithelial cell migration in vitro. *Exp. Cell Res.* **250**: 187–196.
- YARDEN, Y., and M. X. SLIWKOWSKI, 2001 Untangling the ErbB signalling network. *Nat. Rev. Mol. Cell Biol.* **2**: 127–137.
- YUJIRI, T., M. WARE, C. WIDMANN, R. OYER, D. RUSSELL *et al.*, 2000 MEK kinase 1 gene disruption alters cell migration and c-Jun NH2-terminal kinase regulation but does not cause a measurable defect in NF-kappa B activation. *Proc. Natl. Acad. Sci. USA* **97**: 7272–7277.

Communicating editor: N. A. JENKINS